Ultra-low Dose Interleukin-2 Promotes Immune-modulating Function of Regulatory T Cells and Natural Killer Cells in Healthy Volunteers

Sawa Ito[1], Catherine M Bollard[2], Mattias Carlsten[1], Jan Joseph Melenhorst[1,6], Angélique Biancotto[3], Ena Wang[3,4,7], Jinguo Chen[3], Yuri Kotliarov[3], Foo Cheung[3], Zhi Xie[3,8], Francesco Marincola[3,7], Kazushi Tanimoto[1,9], Minoo Battiwalla[1], Matthew J Olnes[1,3,10], Shira Perl[3], Paula Schum[3], Thomas E Hughes[5], Keyvan Keyvanfar[1], Nancy Hensel[1], Pawel Muranski[1], Neal S Young[1,3] and A John Barrett[1]

[1]*Hematology Branch, National Heart, Lung, and Blood Institute, National Institutes of Health, Bethesda, Maryland, USA;* [2]*Children's National Health System and The George Washington University, Washington, District of Columbia, USA;* [3]*Trans-NIH Center for Human Immunology, Autoimmunity and Inflammation, National Institutes of Health, Bethesda, Maryland, USA;* [4]*Department of Transfusion Medicine, Clinical Center, National Institutes of Health, Bethesda, Maryland, USA;* [5]*Pharmacy Department, Clinical Center, National Institutes of Health, Bethesda, Maryland, USA;* [6]*Current address: Department of Pathology and Laboratory Medicine, University of Pennsylvania, Philadelphia, Pennsylvania, USA;* [7]*Current address: Research Branch, Sidra Medical and Research Centre, Doha, Qatar;* [8]*Current address: Zhongshan Ophthalmic Center, Sun Yat-sen University, Guangzhou, China;* [9]*Current address: Department of Hematology, Clinical Immunology and Infectious Disease, Ehime University, Ehime, Japan;* [10]*Current address: Alaska Native Tribal Health Consortium, Anchorage, Alaska, USA*

Low-dose interleukin-2 (IL-2) expands regulatory T cells (T$_{regs}$) and natural killer (NK) cells after stem cell transplantation (SCT) and may reduce graft-versus-host disease (GVHD). We hypothesized that ultra-low dose (ULD) IL-2 could serve as an immune-modulating agent for stem cell donors to prevent GVHD following SCT. However, the safety, dose level, and immune signatures of ULD IL-2 in immune-competent healthy subjects remain unknown. Here, we have characterized the phenotype and function of T$_{regs}$ and NK cells as well as the gene expression and cytokine profiles of 21 healthy volunteers receiving 50,000 to 200,000 units/m²/day IL-2 for 5 days. ULD IL-2 was well tolerated and induced a significant increase in the frequency of T$_{regs}$ with increased suppressive function. There was a marked expansion of CD56^{bright} NK cells with enhanced interferon-γ (IFN-γ) production. Serum cytokine profiling demonstrated increase of IFN-γ induced protein 10 (IP-10). Gene expression analysis revealed significant changes in a highly restricted set of genes, including *FOXP3*, *IL-2RA*, and *CISH*. This is the first study to evaluate global immune-modulating function of ULD IL-2 in healthy subjects and to support the future studies administrating ULD IL-2 to stem cell donors.

INTRODUCTION

Interleukin-2 (IL-2) was originally discovered as a T cell growth factor more than 30 years ago.[1,2] It was the first human cytokine used to boost immune responses in hematologic malignancies and solid tumors[3–6] but with limited clinical benefit and significant toxicity when used in high doses.[7,8] Subsequent *in vivo* and *in vitro* studies have established a role for IL-2 in promoting the development and proliferation of antigen-specific T cells, regulatory T cells (T$_{regs}$), and natural killer (NK) cells.[9] The dual effects of IL-2 on T$_{regs}$ and NK cell have sparked interest in the potential of this cytokine to treat autoimmune disease and graft-versus-host disease (GVHD) after stem cell transplantation (SCT).[9,10] Kennedy-Nasser and Bollard *et al.*[11,12] conducted a clinical protocol of ultra-low dose IL-2 (ULD IL-2: 100,000 to 200,000 IU/m²) early following allogeneic SCT and found a threefold expansion of T$_{regs}$ with no signs of GVHD. Koreth *et al.*[13] reported major responses in patients with steroid refractory chronic GVHD given low-dose IL-2 (LD IL-2: 300,000 to 3,000,000 IU/m²). Recent data further support the use of LD IL-2 to control GVHD by beneficially favoring proliferation, thymic export, and resistance to apoptosis of T$_{regs}$ *in vivo*.[14] We hypothesized that ULD IL-2 could serve as an immune-modulating agent for stem cell donors and transplant recipients, expanding both T$_{regs}$ and NK cells, to prevent GVHD. However, the biological effects of ULD IL-2 in healthy humans are unknown and the optimal dose of the IL-2 for expansion of T$_{regs}$ and NK cells has not been established. Therefore, we studied the immunobiology of T$_{regs}$ and NK cells following administration of three different doses of ULD IL-2 to healthy volunteers. In addition, the dynamic molecular and proteomic changes in response to ULD IL-2 were analyzed to identify the underlying pathways involved in IL-2-mediated homeostasis in immune competent individuals.

RESULTS

ULD IL-2 is well tolerated by healthy volunteers

Twenty-one healthy volunteers (mean age 33; range 22–57, female $n = 9$, male $n = 12$) were enrolled in the study receiving either: 50,000 IU/m²/day ($n = 6$), 100,000 IU/m²/day ($n = 9$), and 200,000

IU/m^2/day (n = 6) of ULD IL-2. All subjects tolerated ULD IL-2 with minimal adverse events, including grade 1 injection site reactions (**Table 1**). No IL-2-related liver or renal toxicities were observed during or after administration. All adverse events completely resolved shortly after the last dose of IL-2. Absolute white blood cell counts were significantly increased at day 4 after initiation of IL-2 (**Supplementary Figure S1a**; P = 0.001) associated with an increase in absolute numbers of neutrophils, monocytes, and eosinophils (**Supplementary Figure S1b, c** and data not shown; P = 0.002, P = 0.008, and P = 0.006, respectively), whereas lymphocyte counts remained unchanged (**Supplementary Figure S1d**; P = 0.249). A subsequent lymphocyte subset analysis demonstrated no significant changes in absolute numbers of CD3$^+$ T cells, CD4$^+$ T cells, CD19$^+$ B cells, and NK cells. Absolute CD8$^+$ T cell counts were slightly decreased at day 4, but this was not statistically significant (P = 0.06) (**Supplementary Figure S1e–h**).

Both Helios positive and negative T$_{regs}$ are expanded by ULD IL-2

We first analyzed the phenotype of T$_{regs}$ and NK cells to evaluate whether ULD IL-2 has an impact on lymphocyte subset composition. The proportion of FoxP3$^+$CD4$^+$ T$_{regs}$ was significantly expanded in all dose cohorts at day 4 (P < 0.0001; **Figure 1a**). In the

Table 1 Characteristics of healthy volunteers

Number of subjects	21	
Mean age (range)	33	(22–57)
Sex, n		
Female	9	
Male	12	
Race, n		
African American	4	
Asian	3	
White	14	
Dose cohort, n		
50,000 IU/m^2/day	6	
100,000 IU/m^2/day	9	
200,000 IU/m^2/day	6	
Adverse events, grade (CECAE v4.0), n		
Injection site reaction	I	19
Injection site reaction	II	1
Fatigue	I	14
Nausea	I	4
Anorexia	I	3
Headache	I	2
Myalgia	I	2
Chills	I	1
Fever	I	1
Flu-like symptoms	I	1
Irritability	I	1
Vomiting	I	1

T$_{regs}$ subset analysis, the proportion of Helios$^+$ T$_{regs}$ was increased by day 2 (P = 0.004; **Figure 1b**), followed by Helios$^-$ T$_{regs}$ that showed an increase first on day 3 (P = 0.01; **Figure 1c**). Both subsets of T$_{regs}$ significantly expanded, peaking at day 4 and remaining higher than baseline at least until day 7. Expansion of Helios$^+$T$_{regs}$ was primarily observed in the 100,000 and 200,000 IU/m^2 IL-2 dose cohorts, whereas healthy donors treated with 50,000 IU/m^2 showed modest Helios$^+$T$_{regs}$ mobilization (**Figure 1d**). *In vivo* proliferation of Helios$^+$ T$_{regs}$ was confirmed by changes in Ki67 expression preferentially in the 100,000 and 200,000 IU/m^2 dose cohorts but not observed in 50,000 IU/m^2 dose cohort (**Figure 1e**). HLA-DR expression was significantly increased in FoxP3$^+$T$_{regs}$ specifically in the Helios$^+$T$_{regs}$ subset, peaking at day 3 which implies functional activation of T$_{regs}$. HLA-DR induction was more prominent in 200,000 IU/m^2 cohort compared to the 50,000 or 100,000 IU/m^2 cohorts (**Figure 1f**).

CD56^{bright} NK cells are preferentially expanded by ULD IL-2

In concordance with the T$_{regs}$ data, the proportion of CD56^{bright} NK cells among total circulating NK cells increased at day 7 (P < 0.0001; **Figure 2a**), whereas the more mature CD56^{dim}NKG2A$^+$KIR$^-$ and CD56^{dim}KIR$^+$CD57$^+$ NK cell subsets remained around baseline (data not shown). The Ki67 proliferation marker further verified a significant *in vivo* proliferation of NK cells at day 4 (**Figure 2b**) especially within the subset of CD56^{bright} NK cells compared to CD56^{dim}NKG2A$^+$KIR$^-$ and CD56^{dim}KIR$^+$CD57$^+$ NK cell populations (P < 0.0001; **Figure 2c**). Expansion of CD56^{bright} NK cell subset was dose dependent with the most prominent expansion observed at dose level of 200,000 IU/m^2 (**Figure 2d**).

T$_{regs}$ and NK cell function are augmented by ULD IL-2

To determine if IL-2-inducible T$_{regs}$ and NK cell retain their functions, we next evaluated the *in vitro* T$_{regs}$ suppression capacity and NK cell cytokine production comparing in paired samples from the same subject before and after IL-2 administration. Conventional T cells (T$_{cons}$: CD3$^+$CD4$^+$CD25^{low}CD127^{high}) equally expressed CD154 following stimulation with anti-CD3/CD28-coated beads in pre- and post-IL-2 samples (P = 0.86) suggesting ULD IL-2 did not affect T cell receptor–mediated activation of T$_{cons}$ (**Figure 3a**). The suppressive capacity of T$_{regs}$ on CD154 activation of autologous T$_{cons}$ was significantly increased in post-IL-2 samples at a T$_{regs}$:T$_{cons}$ ratio 1:1 (P = 0.02; **Figure 3b**). NK cell functional analysis demonstrated significantly increased IFN-γ production following cytokine stimulation of CD56^{bright} NK cells post-IL-2 compared to pre-IL-2 (P = 0.009; **Figure 3c**), whereas no such effect was observed following stimulation with K562 cells. No difference was observed for CD107a expression by CD56^{dim} NK cells following coculture with K562 or cytokine stimulation when comparing samples collected before and after IL-2 injection (P = 0.75; **Figure 3d**). These findings indicate that ULD IL-2 not only expanded but also preferentially augmented the function of T$_{regs}$ and CD56^{bright} NK cell.

IP-10 is increased after ULD IL-2

To determine if ULD IL-2 alters proteomic profiles, 76 cytokines, chemokines, acute phase proteins, and diabetes panel proteins were measured in plasma samples (**Supplementary Table S1**).
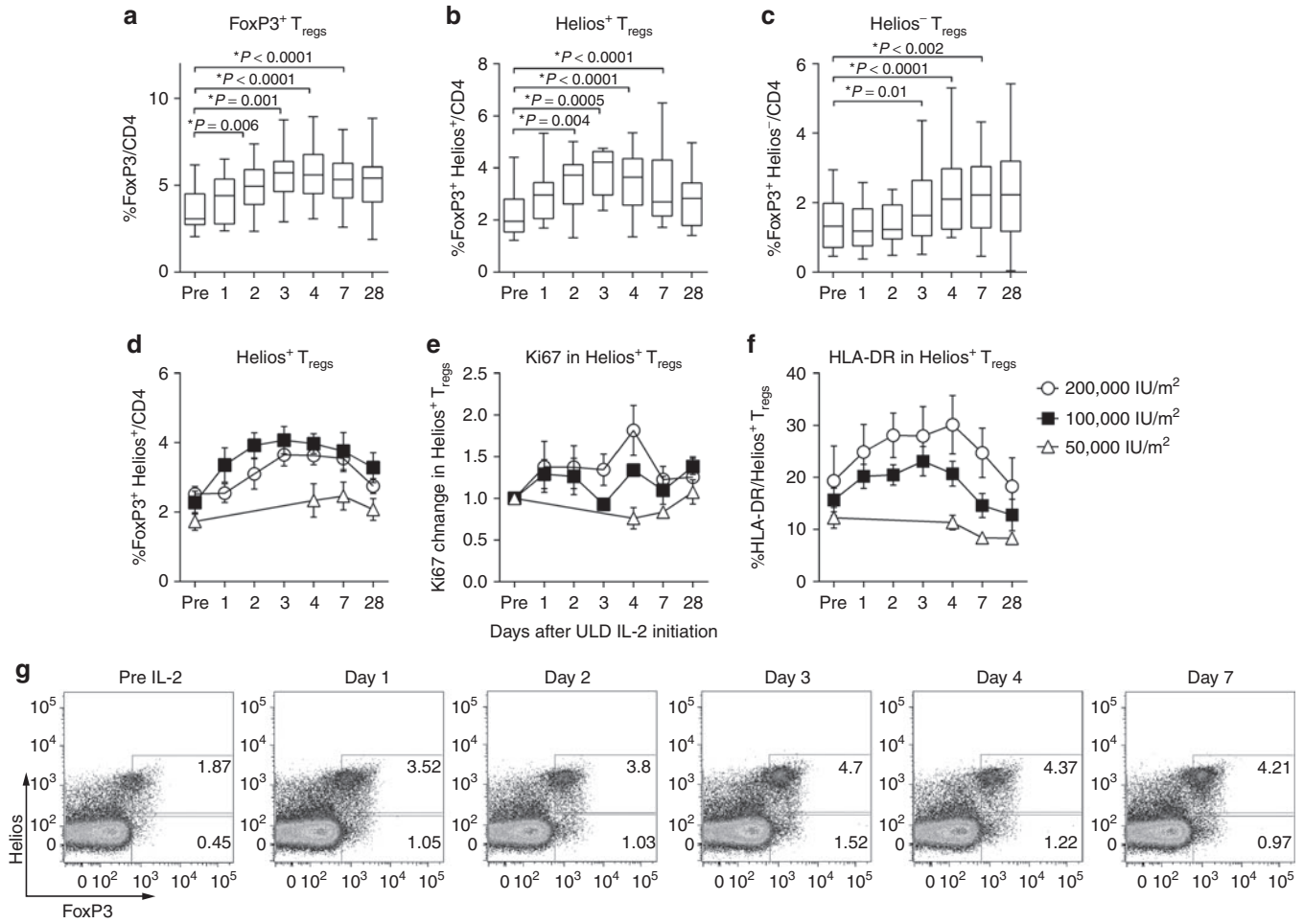
Figure 1 Chronological changes in T$_{regs}$ subsets after ultra-low dose (ULD) IL-2. (a) %FoxP3$^+$CD4 T$_{regs}$ were significantly increased and peaked at day 4 (mean 3.53±1.17% at day 0 versus 5.68±1.56% at day 4; $P < 0.0001$). **(b,c)** Helios$^+$FoxP3$^+$T$_{regs}$ were significantly increased by day 2 (mean 2.19±1.17% at day 0 versus 3.51±1.03% at day 2; $P = 0.004$) followed by Helios$^-$FoxP3$^+$T$_{regs}$ (mean 1.36±0.71% at day 0 versus 1.86±1.16% at day 3; $P = 0.01$). Both subsets of T$_{regs}$ significantly expanded, peaking at day 4 and remaining significantly higher than baseline until day 7. **(d)** Expansion of Helios$^+$FoxP3$^+$T$_{regs}$ was significantly higher when donors received 100,000 and 200,000 IU/m^2 IL-2 compared to 50,000 IU/m^2 ($P < 0.001$ and $P = 0.01$ at day 4 respectively). **(e)** Ki67 was significantly induced in Helios$^+$FoxP3$^+$T$_{regs}$ specifically in 100,000 and 200,000 IU/m^2 IL-2 compared to 50,000 IU/m^2 ($P = 0.03$ and $P = 0.01$ at day 4 respectively). **(f)** HLA-DR was significantly induced in Helios$^+$FoxP3$^+$T$_{regs}$ specifically in 100,000 and 200,000 IU/m^2 IL-2 compared to 50,000 IU/m^2 ($P = 0.008$ and $P = 0.04$ at day 4 respectively). **(g)** The representative flow cytometry data showed expansions of FoxP3$^+$CD4 T$_{regs}$ in both Helios fractions in healthy volunteer receiving ULD IL-2 (200,000 IU/m^2).
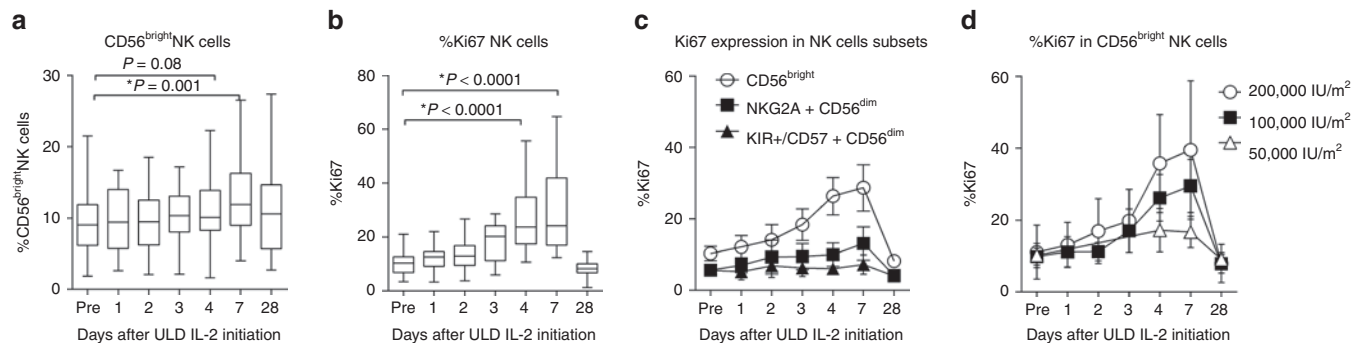

Figure 2 Chronological changes in natural killer (NK) cell subsets after ultra-low dose (ULD) IL-2. (a) CD56^{bright} NK cells were significantly increased at day 7 (9.0±4.7% at day 0 versus 12.7±5.8% at day 7; $P = 0.001$). **(b)** %Ki67 in NK cell was markedly increased at day 4 ($P < 0.0001$). **(c,d)** %Ki67 was significantly induced in CD56^{bright} NK cells compared to CD56^{dim}NKG2A$^+$KIR$^-$, and CD56^{dim}KIR$^+$CD57$^+$ NK populations (26.4±11.4% Ki67$^+$ in CD56^{bright} NK, versus 10.1±7.3% in CD56^{dim}NKG2A$^+$KIR$^-$NK, 6.1±2.9% CD56^{dim}KIR$^+$CD57$^+$ NK at day 4; $P < 0.0001$) especially in the cohort of 200,000 IU/m^2.
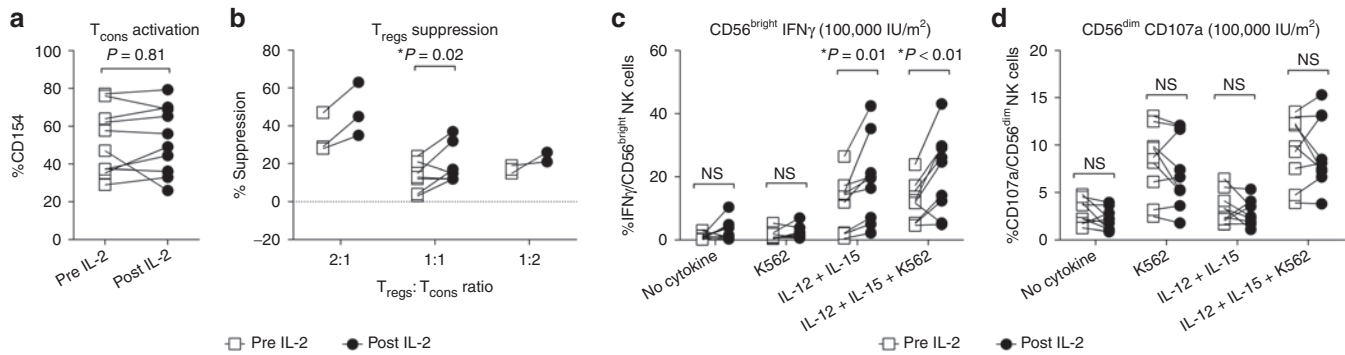
Figure 3 *In vitro* functions of T_{regs} and natural killer (NK) cells after ultra-low dose (ULD) IL-2. (**a**) T_{cons} (CD3⁺CD4⁺CD25^{low}CD127^{high}) equally expressed CD154 through anti-CD3/CD28-coated bead stimulation in pre- and post-IL-2 samples (CD154 expression 52.3±17.5% pre-IL-2 T_{cons} versus 52.8±17.9% post-IL-2 T_{con}; $P = 0.86$). (**b**) The suppressive capacity of T_{regs} on CD154 activation of autologous T_{cons} was significantly increased in post-IL-2 samples (% suppression 14.0±6.9% pre-IL-2 versus 19.9±8.8% post-IL-2 at T_{regs}:T_{cons} ratio 1:1; $P = 0.02$). (**c**) Significantly increased interferon (IFN)-γ productions in post-IL-2 NK cells was observed compared to pre-IL-2 NK cells especially in the CD56^{bright}NK cell subset (mean %IFN-γ production 12.0±2.1% pre-IL-2 versus 21.0±4.2% post-IL-2 with IL-12+IL15 and K562 stimulation; $P = 0.009$). (**d**) CD107a expression was not significantly different pre- versus post-IL-2 injections (mean %CD107a expression in CD56^{dim}NK cells, 9.6±3.6% pre-IL-2 versus 9.3±3.7% post-IL-2 with IL-12+IL15 and K562 stimulation; $P = 0.75$).

Wilcoxon signed-rank test after false discovery rate (FDR) correction demonstrated a significant increase in circulating level of IFN-γ induced protein 10 (IP-10/CXCL10, a ligand for CXCR3) from day 2 through 4 (**Supplementary Figure S2**). In contrast, circulating levels of other cytokines including IL-2, IFN-γ, IL-6, IL-10, IL-15, and IL-17 remained unchanged. This finding suggests a highly specific biological effect of ULD IL-2.

CISH, IL-2RA, and FoxP3 expression are preferentially upregulated by ULD IL-2

Gene expression microarray was performed to identify the different expression profiles in response to the three doses of IL-2 administered to healthy donors. The expression profile of peripheral whole blood before and 4 and 7 days after the first dose of IL-2 ($n = 21$) was compared using a paired t-test with two-tailed P_2 value less than 0.05 corrected by FDR for multiple testing. Four days after the first dose of ULD IL-2, only 10 genes were significantly differentially expressed compared to pre-ULD IL-2 (**Figure 4a**; **Supplementary Table S2**). Nine genes were significantly upregulated: *CISH*, *FoxP3*, *IL2RA*, *CTLS1*, *STAT1*, *GBP1*, *CASP4*, *IRF9*, *IFITM3*, whereas only one gene, *ANKRD37*, was significantly downregulated. On day 7 after IL-2 administration, 14 genes were differentially expressed including *IL2RA* which remained significantly upregulated 3 days after the last dose of ULD IL-2. Samples from 12 subjects (100,000 and 200,000 IU/m², $n = 6$ respectively) were available for further time-course analysis comparing pre- and day 1, 2, 3, 4, and 7 after the first dose of IL-2. The kinetics of expression profiles revealed that *FoxP3* and *IL2RA* were significantly upregulated as early as 2 days through 4 days after the first dose of IL-2 suggesting they represented the most sensitive genes responding to ULD IL-2 (**Figure 4b**).

Thirty-three gene sets were significantly enriched with genes differentially expressed by ULD IL-2 on day 4 ($P < 0.005$). The gene sets include both innate and adoptive immunity-related pathways. Pathways related to hematopoiesis such as Granulocyte-macrophage colony-stimulating factor signaling and JAK-Stat

signaling were also significantly enriched, consistent with the finding of increased neutrophil and monocyte counts and suggesting ULD IL-2 also targets a broad spectrum of genes outside T_{regs} and NK cells (**Supplementary Table S3**). To annotate functional interpretation of the differentially expressed genes by ULD IL-2, we used Ingenuity Pathway Analysis software to compare pre- and day 4 post-ULD IL-2 datasets. Genes modified by ULD IL-2 were significantly enriched in 33 functional categories ($P < 0.05$) including hematological system development and function, and immune cell trafficking (**Supplementary Table S4**). In canonical pathway analysis, 29 pathways were enriched in the ULD IL-2 gene set. Gene sets predominantly upregulated by ULD IL-2 occurred in IL-9 signaling, T helper cell differentiation, and interferon signaling, suggesting that ULD IL-2 primarily affects immune-regulating genes. Gene sets predominantly downregulated by ULD IL-2 were found in systemic lupus erythematosus signaling (**Supplementary Table S5**).

DISCUSSION

This is the first study to prospectively evaluate the global immune signatures of ULD IL-2 in healthy volunteers. ULD IL-2 significantly expanded T_{regs} in immune-competent healthy volunteers in a similar way to immune-compromised hematopoietic stem cell transplant recipients and cancer patients.[5,6,13–15] We further characterized T_{regs} subset by Helios, a transcription factor which was previously proposed as a marker of thymus derived T_{regs}.[16] The proposal has been challenged by serial observations reporting Helios may represent the activation or proliferation marker of T_{regs}[17] and can be acquired by peripherally induced T_{regs}.[18] Most recent data, however demonstrated that majority of T_{regs} were composed by Helios⁺T_{regs} in human thymus, cord blood, and at the time of engraftment after allo-SCT favoring the hypothesis that Helios⁺T_{regs} can be useful marker for thymus-induced T_{regs} in clinical settings.[19–22] In our study, both Helios-positive and Helios-negative T_{regs}, were equally expanded by ULD IL-2. Ki67 expression supported *in vivo* proliferation of both Helios⁺T_{regs} and HLA-DR expression suggested *in vivo* activation of Helios⁺T_{regs}.
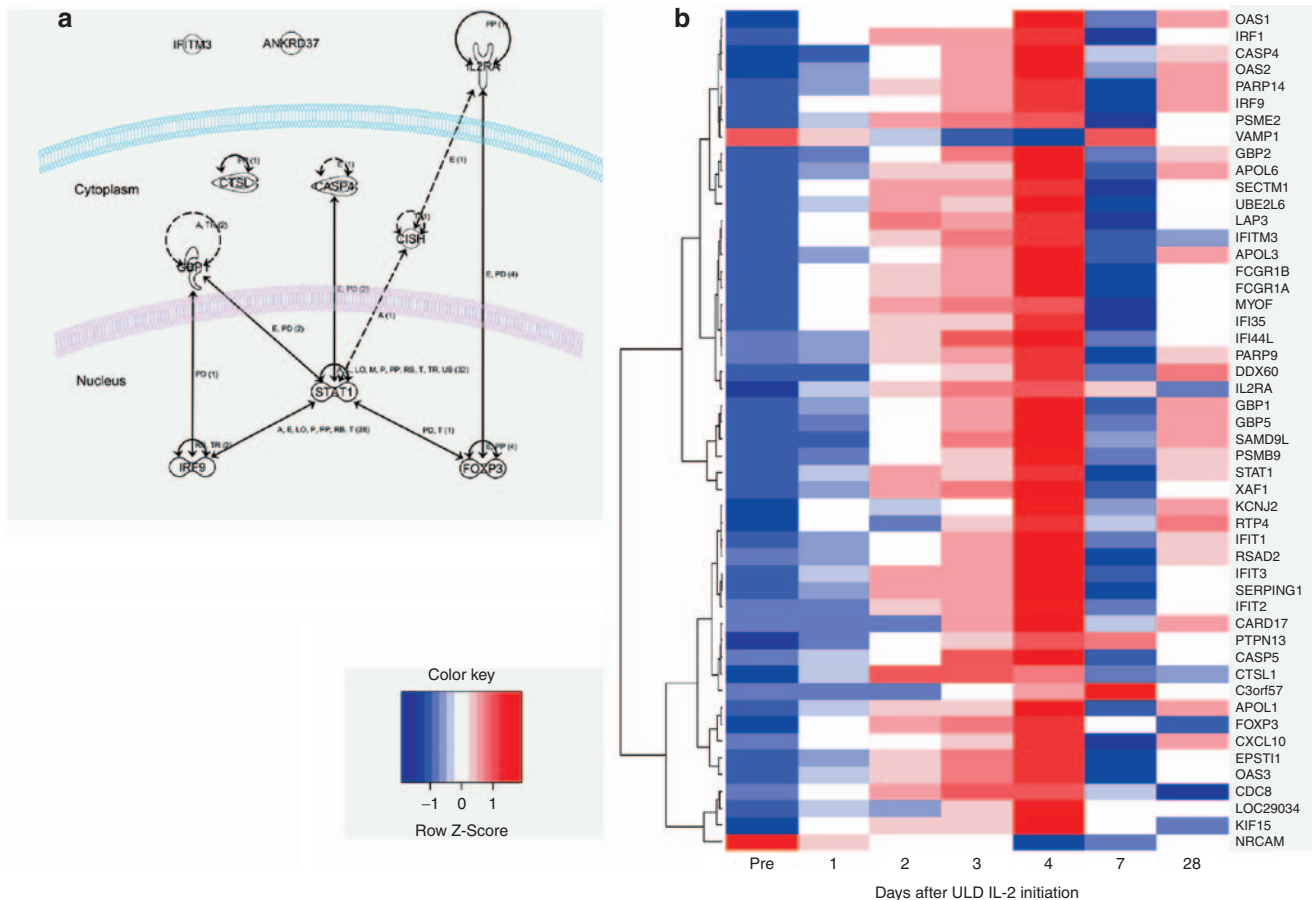
Figure 4 Genes differentially expressed by ultra-low dose (ULD) IL-2 in healthy volunteers. (a) Functional annotation of ULD IL-2 related genes: functional relationships are annotated to the genes differentially expressed on day 4 after ULD IL-2 using IPA Ingenuity Path Designer. **(b)** Time-course analysis of differentially expressed genes after ULD IL-2: hierarchical clustering of genes differentially expressed after ULD IL-2 is shown in a heatmap. Days are represented in the columns and probe sets in the rows.

In vitro function assay demonstrated that T_{regs} recovered from treated subjects were capable of suppressing autologous T_{cons} activation, confirming that ULD IL-2 indeed augmented their biological activity. Our findings further support the fact that IL-2 is critically important for T_{regs} homeostasis.[23] The mechanism of selective T_{regs} expansion by ULD IL-2 may be explained by two scenarios[24]: preferential IL-2 consumption by T_{regs} induces cytokine deprivation-mediated apoptosis in T_{cons}[25]; and/or that highly sensitive intrinsic IL-2R signaling provides T_{regs} survival advantages over T_{cons} cell within thymic or peripheral tissues where available IL-2 is normally limited.[26]

NK cell subset analysis revealed increased Ki67 expression within the CD56^{bright} NK cell compartment following ULD IL-2, rather than within the more differentiated NK cell subsets such as CD56^{dim}NKG2A^{+}KIR^{−} and CD56^{dim}KIR^{+}CD57^{+} NK cells.[27,28] *In vitro* analysis further demonstrated that expanded CD56^{bright} NK cells retained functionality, as they produced IFN-γ. CD56^{bright} NK cells are considered more immature than CD56^{dim} NK cells and are known to express the high affinity IL-2 receptor.[29] In pioneering work by Fehniger *et al.*,[4] LD IL-2 significantly expanded CD56^{bright} NK cells in patients with acute myeloid leukemia. The mechanism of selective expansion of this particular NK cell subset was hypothesized to result from enhanced differentiation from bone marrow progenitors residing in secondary lymphoid tissues.[4,30] A recent *in vivo* model demonstrated the preferential accumulation of immature NK cells at the site of inflammation in tumor-bearing and chronically infected mice.[31,32] IFN-γ produced by NK cell is known to promote antimicrobial immunity through the maturation of dendritic cells and the induction of T helper cell type 1 ($T_{H}1$) responses.[33,34] Therefore, CD56^{bright} NK cells induced by ULD IL-2 may have a beneficial effect to promote antimicrobial immunity, although the exact role of CD56^{bright} NK cells in antitumor activity is unclear.

Most recently, a crosstalk between T_{regs} and NK cell in the context of IL-2 biology has been reported in several mouse models.[32,35,36] Sitrin *et al.*[36] proposed that T_{regs} function as a cytokine sink, depriving NK cell of IL-2. Gasteiger *et al.*[32] also demonstrated that T_{regs} restrain the expansion and maturation of immature NK cell in an IL-2-dependent manner. The immune-phenotypic changes observed in our study suggest a similar crosstalk between T_{regs} and CD56^{bright} NK cell. Importantly, our *in vitro* function analysis showed cytokine production and cytotoxicity were not impaired in NK cells isolated after ULD IL-2 administration from PBMC, which also contained expanded T_{regs}. Further research in T_{regs}-NK cell crosstalk in healthy individuals is needed to clarify the pathways involved.

In order to investigate underlying pathways of ULD IL-2 for this distinct immune-phenotype, we performed a comprehensive cytokine profiling in serum and gene expression microarrays in PBMC. Strikingly, cytokine analysis found only a significant increase in the level of IP-10 (or CXCL10), a chemokine known to be induced by IFN-γ acting as a chemoattractants for monocytes, T cells (including T_H1 cells) and NK cells via CXCR3 receptor. IP-10 (CXCL10) is a biomarker associated with various diseases including tuberculosis, autoimmune disease, hepatitis C, and solid organ transplantation.[37,38] Recent data suggest that IP-10 (CXCL10) is an important chemoattractant for NK cells, sustaining antitumor effects of IL-2 in a mouse model.[39] Thus, ULD IL-2 administration induces a very specific type 1-related immune effect *in vivo*. Similarly, striking was the finding that gene expression profiling identified only a highly restricted set of 10 transcriptomes differentially expressed after administration of ULD IL-2, considerably fewer than the results of microarray analysis reported in melanoma patients receiving high-dose IL-2.[40,41] Notably, the selective coinduction of *FoxP3* and *IL2RA* as early as 2 days after ULD IL-2 was a unique feature in our study and compatible with the immune-phenotype profiles of expanding T_{regs} defined by IL2RA (CD25)^{high} and FoxP3$^+$ cells. *CISH*, known to be upregulated by IL-2 *in vitro* was another distinct gene significantly upregulated after ULD IL-2. CISH is a cytokine inducible SRC homology 2 (SH2) domain protein and belongs to a member of the suppressor of cytokine signaling (SOCS) family which plays an important role in the negative feedback of human cytokine signal transduction. Polymorphisms of *CISH* gene are associated with the susceptibility to various infectious diseases including bacteremia, malaria, and tuberculosis.[42] *STAT1*, *IRF9*, *GBP1*, and *IFITM3* are all associated with IFN-γ and gene set enrichment analysis identified that ULD IL-2 activated pathways in the domain of IRF by cytosolic pattern recognition receptors, T helper cell differentiation, and interferon signaling suggesting an activation of type 1-related immune response. In contrast, ULD IL-2 was associated with significant downregulation of genes enriched in systemic lupus erythematosus signaling, suggesting a potential immune-modulating function of ULD IL-2 in autoimmune disease. This gene expression profile pattern implies that ULD IL-2 has two paradoxical but complementary functions: to promote innate and adoptive immunity by IFN-γ signaling and to induce immune suppressive function through FoxP3$^+$T$_{regs}$. These functions help to maintain the homeostasis of the immune system in response to infectious pathogens, while preventing resultant excessive autoimmunity.[24] Our data are limited to analyze the net effect of ULD IL-2 in whole blood gene expression profile of healthy donors. Gene expression profiles in sorted T_{regs}, NK cells, and other immune cell compartments would provide further insights of the differential effects of ULD IL-2 in future study.

The immune-modulating properties of ULD IL-2 clearly distinguish it from "conventional" immunosuppressive agents used for hematopoietic SCT, solid organ transplantation, and autoimmune diseases. ULD IL-2 modulates the immune system to restore its normal homeostasis[14] rather than generally suppressing the immune system, with the concurrent risk of infectious complications. Most clinical trials have used considerably higher doses of IL-2, and there has hitherto been a lack of information on the relationship between dose and immune-modulating function of ULD IL-2 in man. Our study now defines a lower limit of biological function of subcutaneously administered IL-2 in the region of 100,000 and 200,000 IU/m². This should guide dose selection for ULD IL-2 in future clinical studies. In the setting of hematopoietic SCT, these results provide the rationale to administer ULD IL-2 in SCT donors to prevent GVHD by increasing T_{regs} in the stem cell graft. Furthermore, promoting CD56^{bright} NK cell function by ULD IL-2 may reduce the risk of opportunistic infections. Several questions will need to be addressed in a future clinical trial: (i) what is the optimal *in vivo* expansion and activation of T_{regs} and NK cells required? (ii) How can we maintain *in vivo* expanded and activated T_{regs} and NK cells after adoptive transfer? (iii) What is the impact of T_{regs} and CD56^{bright} NK cells on antitumor effects? Also the activation of type 1 immune response-related genes parallel to immune suppression genes, *FoxP3* and *CISH* in gene expression microarray analysis may raise the concern of efficacy of ULD IL-2 primed donor graft in GVHD prophylaxis. Nevertheless, the safety profile in healthy individuals determined in this study opens the possibility of administrating ULD IL-2 to donors in settings of well-designed clinical study targeting high GVHD risk SCT such as haploidentical donor SCT.

MATERIALS AND METHODS

Healthy volunteer study. A phase 1, single-center trial was conducted to evaluate the safety and tolerability of ULD IL-2 in healthy volunteers from December 2011 to April 2013 (NIH protocol 11-H-0268: NCT01445561). Written informed consent including the use of samples for research was obtained from eligible healthy volunteers in accordance with Declaration of Helsinki and the Institutional Review Board of the National Heart, Lung, and Blood Institute, NIH. IL-2 (Aldesleukin, Proleukin; Prometheus Laboratories, San Diego, CA) was reconstituted in sterile water for injection, USP and further diluted in 5% dextrose in water, USP to a concentration of 200 μg/ml. Each daily dose was prefilled in a 0.5-ml tuberculin syringe. Enrolled subjects received IL-2 by subcutaneous injection once a day for 5 consecutive days. The study consisted of three dosing cohorts, 50,000, 100,000, and 200,000 IU/m². Adverse events were monitored daily, and both clinical and laboratory toxicity were graded according to National Cancer Institute Common Terminology Criteria for Adverse Events (NCI-CTCAE) version 4.03.

Sample collection and storage. Serial blood samples were collected before and 1, 2, 3, 4, 7, and 28 days after initial IL-2 injection in first two dose cohorts (100,000 and 200,000 IU/m²). In subsequent cohorts, which included the 50,000 IU/m² dose level, samples were collected before and 4, 7, and 28 days after initial IL-2 injection. Peripheral blood mononuclear cells (PBMC) were isolated by Ficoll-Hypaque density gradient centrifugation (Organon Teknika, Durham, NC) and cryopreserved in RPMI-1640 (Life Technologies, Gaithersburg, MD) supplemented with 20% heat-inactivated fetal bovine serum (Sigma-Aldrich, St Louis, MO) and 10% dimethyl sulfoxide according to standard protocol. Serum was obtained by centrifugation of peripheral blood collected in serum separating tubes (SST) (Beckton Dickinson, San Jose, CA). PBMC and plasma samples were stored in liquid nitrogen and −80 °C freezer respectively until further use.

Immunophenotyping by flow cytometry. PBMC samples from all 21 subjects at all time points were available for analysis. Before use, cells were thawed and washed in RPMI 1640 supplemented with 10% FCS. Cells were stained with violet dead cell-exclusion dye (ViViD; Invitrogen, Molecular Probes, Eugene, OR) and a monoclonal antibody (mAb) panel designed to identify T_{regs} and NK cell subsets. The following mAb and fluorescent dyes were used: CD3-Brillant Violet 605 (clone OKT3),

CD8-Brilliant Violet 570 (clone RPA-T8), CD31-PECy7 (clone WM59), CD45RA-APCCy7 (clone HI100), CD57-APC (clone HCD57), CD127-Brilliant Violet 650 (clone A019D5), KIR3DL1-Alexa Fluor 700 (clone DX-9), Helios-PE (clone 22F6) from Biolegend, San Diego, CA; ViViD amine reactive dye (ViViD: LIVE/DEAD fixable violet dead cell stain), CD14-Pacific Blue (clone TüK4), CD19-Pacific Blue (clone SJ25-C1) from Invitrogen; CD27-PECy5 (clone 1A4CD27), NKG2A-PE (clone z199), KIR2DL2/3-PECy5.5 (clone EB6B), KIR2DL3/3-PECy5.5 (clone GL183) from Beckman Coulter, Brea, CA; CD4-V500 (clone RPA-T4), CD16-V500 (clone 3G8), CD45RO-APCH7 (clone UCHL1), CD56-PECy7 (clone NCAM16.2), CD95-APC (clone DX2), CD197-Alexa Fluor 700 (clone 150503), HLA-DR PerCPCy5.5 (clone L243), Ki67-FITC (clone B56) from BD Bioscience (Franklin Lakes, NJ); FoxP3-Alexa Fluor 647 (clone 236A/E7) from eBioscience (San Diego, CA). T_{regs} subsets were determined within the CD4$^+$ T cell population to identify Helios$^+$T$_{regs}$: CD4$^+$FoxP3$^+$Helios$^+$ and Helios$^-$ T$_{regs}$: CD4$^+$FoxP3+Helios$^-$.[16,43] NK cell subsets were determined within CD56$^+$CD3$^-$ population using NKG2A, KIR2DL1, KIR2DL2/3, KIR3DL1, and CD57 to identify CD56^{bright}, CD56^{dim}NKG2A$^+$KIR$^-$, and CD56^{dim} KIR$^+$CD57$^+$ NK cells.[27,28] Data acquisition was performed using a Becton Dickinson LSRII Fortessa, and data were analyzed using FlowJo software (Tree Star, Ashland, OR). At least 50,000 events per CD4$^+$, CD8$^+$ or CD56$^+$CD3$^-$ cell population were acquired to ensure a sufficient number of cells for statistical analysis.

Tregs and NK cell function assays. Paired PBMC samples before and 4 days after IL-2 administration from the 50,000 and 100,000 IU/m^2 cohorts ($n = 12$) were used to evaluate the function of T_{regs} and NK cells *in vitro*. PBMCs were labeled with mAbs against CD4, CD25, CD56, CD127, CD14, CD19, CD3, and propidium iodide (Molecular Probe, Eugene, OR). T_{regs} (CD3$^+$CD4$^+$CD25^{high}CD127^{low}), conventional T cells (T$_{cons}$: CD3$^+$CD4$^+$CD25^{low}CD127^{high}), and NK cells (CD56$^+$CD3$^-$) were sorted in propidium iodide-negative (viable) population on FACS Aria II cell sorter (BD, Franklin Lakes, NJ). Sorting purity for FoxP3$^+$ cells in sorted T_{regs} was more than 90%. For T_{regs} suppression assay, T_{cons} were stained with CellTrace Violet (CTV, Life Technologies, Carlsbad, CA) according to manufacturer's instruction and were then stimulated with anti-CD3/CD28-coated beads (Dynabeads; Invitrogen, Carlsbad, CA) at a bead/T_{cons} ratio of 0.1:1. 20,000 T_{cons} were then incubated with T_{regs} at the ratio of 1:1 to 1:2 (responder: suppressor). Anti-CD154 was added at time of incubation ($t = 0$). After incubation at 37 °C in 5%CO$_2$ for 16 hours, cells were acquired on LSRII Fortessa Cytometer (BD). The proportion of CD154 expression was measured within CTV-labeled T$_{cons}$, and the percentage suppression of CD154 was calculated using the formula: %Suppression = $100 - (a/b \times 100)$ where a is percentage positive CD154 T$_{cons}$ in the presence of T_{regs} and b is percentage positive in the absence of T_{regs}.[44] For NK cell function analysis, sorted NK cells ($0.5-1 \times 10^5$) were mixed with an equal number of CTV-labeled K562 cells and/or cytokine stimulation (IL-12 10 ng/ml; IL-15 100 ng/ml) and Brefeldin A (GolgiPlug; BD Bioscience).[45] After 6 hours incubation at 37 °C in 5%CO$_2$, cells were stained for extracellular expression of CD3, CD56, CD57, CD107a, KIR2DL2/3, KIR2DL3/3 as well as with the ViViD viability dye. Thereafter, cells were permeabilized (Cytofix/Cytoperm Buffer; BD Biosciences) and stained for IFN-γ. Cells were analyzed on a LSR II Fortessa Cytometer.

Cytokine analysis. Seventy-six human cytokines, chemokines, acute phase proteins, and diabetes panel proteins were analyzed using human cytokine multiplexing panel kits (Bio-Rad, Hercules, CA). All assays were performed according to Bio-Rad kit protocols. Median fluorescence intensities were measured on Luminex 100 instrument (Luminex; Bio-Rad). Standard curves for each cytokine were generated using the premixed lyophilized standards provided in the kits. Cytokine concentrations in samples were determined from the appropriate standard curve using a 5 point-regression to transform mean fluorescence intensities into concentrations using Bio-Plex Manager software version 6. Each sample was run in duplicate, and the average of the duplicate was used as the measured concentration.

Gene expression profiling. Total RNA was extracted from PBMC using a miRNeasy kit (Qiagen, Valencia, CA). Universal RNA quality and quantity was estimated using Nanodrop (Thermo Scientific, Wilmington, DE) and Agilent 2100 Bioanalyzer (Agilent Technologies, Palo Alto, CA). RNA was amplified from 300 ng of total RNA (Ambion WT Expression Kit; Affymetrix, Santa Clara, CA). cDNA was reverse transcribed with biotinylation and hybridized to the GeneChip Human Gene 1.0 ST Arrays (Affymetrix WTTerminal Labeling Kit; Affymetrix) after fragmentation. The arrays were washed and stained on a GeneChip Fluidics Station 450 (Affymetrix); scanning was carried out with the GeneChip Scanner 3000 and image analysis with the Affymetrix GeneChip Command Console Scan Control.

Statistical analysis. The data from immunophenotyping and functional assays were analyzed with Prism Version 5.04 (GraphPad Sotfware, La Jolla, CA). Statistical significance was accepted if the *P* value was <0.05 based on one-way analysis of variance and Wilcoxon matched-pairs signed rank test. Affymetrix CEL files were processed with Affymetrix Power Tools for probeset summarization, normalization, and log2-transformation (RMA with sketch quantile normalization). Quality assessment was conducted using R/Bioconductor package "arrayQualityMetrics",[46] and no outlying arrays were found. Array hybridization data were found to be significantly correlated with most probe sets and its effect was removed using linear regression with R "limma" package.[47] Prior to further analysis, probesets without annotated gene symbol (using the latest NetAffx annotation) as well as probesets with very low variation (with interquantile range less than 0.15) were filtered out. In addition, probesets associated with multiple genes were also removed. In the case of genes associated with multiple probesets, only one probeset, having the best correlation with first principal component for those probesets across all the samples, was selected (in-house developed R function). After all filtering steps, 15,193 genes were left. To determine genes changing expression from day 0 coherently across individuals, the R/Bioconductor package "limma"[47] was used. Subject IDs were included in the model to ensure pair-wise comparison between time points and day 0. *P* values were adjusted for multiple testing using Benjamini and Hochberg's method to estimate the FDR.[48] Stringent cutoffs of 5% FDR-adjusted *P* value and 0.1 log2-fold-change were used to identify differentially expressed genes. Ingenuity Pathway Analysis software (Ingenuity Systems, Redwood City, CA) was used for functional interpretation of gene expression data. Coherent changes in cytokine concentration were analyzed utilizing in-house developed web tool with Perl and R used at the backend. Cytokines with significant response were identified with cutoff of 5% FDR-adjusted *P* values from Wilcoxon signed rank test.

SUPPLEMENTARY MATERIAL
Figure S1. Chronological changes in absolute peripheral blood counts after ULD IL-2.
Figure S2. Changes in serum IP-10 level after ULD IL-2.
Table S1. 76 analytes measured in serum cytokine profiling.
Table S2. Genes differentially expressed after ULD IL-2 in healthy volunteers.
Table S3. Gene sets significantly enriched with genes differentially expressed by ULD IL-2 on day 4.
Table S4. Top functional categories of differentially expressed genes.
Table S5. Top canonical pathways of differentially expressed genes.

REFERENCES

1. Morgan, DA, Ruscetti, FW and Gallo, R (1976). Selective *in vitro* growth of T lymphocytes from normal human bone marrows. *Science* **193**: 1007–1008.
2. Smith, KA (1988). Interleukin-2: inception, impact, and implications. *Science* **240**: 1169–1176.
3. Macdonald, D, Jiang, YZ, Gordon, AA, Mahendra, P, Oskam, R, Palmer, PA *et al.* (1990). Recombinant interleukin 2 for acute myeloid leukaemia in first complete remission: a pilot study. *Leuk Res* **14**: 967–973.
4. Fehniger, TA, Bluman, EM, Porter, MM, Mrózek, E, Cooper, MA, VanDeusen, JB *et al.* (2000). Potential mechanisms of human natural killer cell expansion *in vivo* during low-dose IL-2 therapy. *J Clin Invest* **106**: 117–124.
5. Ahmadzadeh, M and Rosenberg, SA (2006). IL-2 administration increases CD4+ CD25(hi) Foxp3+ regulatory T cells in cancer patients. *Blood* **107**: 2409–2414.
6. Sim, GC, Martin-Orozco, N, Jin, L, Yang, Y, Wu, S, Washington, E *et al.* (2014). IL-2 therapy promotes suppressive ICOS+ Treg expansion in melanoma patients. *J Clin Invest* **124**: 99–110.
7. Atkins, MB, Lotze, MT, Dutcher, JP, Fisher, RI, Weiss, G, Margolin, K *et al.* (1999). High-dose recombinant interleukin 2 therapy for patients with metastatic melanoma: analysis of 270 patients treated between 1985 and 1993. *J Clin Oncol* **17**: 2105–2116.
8. Rosenberg, SA, Yang, JC, Topalian, SL, Schwartzentruber, DJ, Weber, JS, Parkinson, DR *et al.* (1994). Treatment of 283 consecutive patients with metastatic melanoma or renal cell cancer using high-dose bolus interleukin 2. *JAMA* **271**: 907–913.
9. Dooms, H and Abbas, AK (2010). Revisiting the role of IL-2 in autoimmunity. *Eur J Immunol* **40**: 1538–1540.
10. Shevach, EM (2012). Application of IL-2 therapy to target T regulatory cell function. *Trends Immunol* **33**: 626–632.
11. Kennedy-Nasser, AA, Ku, S, Melenhorst, J, Barrett, J, Hazrat, Y, Durett, AG, *et al.* (2012). Ultra low-dose IL-2 mediated expansion of regulatory T cells as GvHD prophylaxis for recipients of allogeneic hematopoietic stem cells. ASBMT Tandem Meeting 2012.
12. Kennedy-Nasser, AA, Ku, S, Castillo-Caro, P, Hazrat, Y, Wu, M-F, Liu, H, *et al.* (2014). Ultra low-dose IL-2 for GVHD prophylaxis after allogeneic hematopoietic stem cell transplantation mediates expansion of regulatory T cells without diminishing antiviral and antileukemic activity. *Clin Cancer Res.* **20**: 2215–2225.
13. Koreth, J, Matsuoka, K, Kim, HT, McDonough, SM, Bindra, B, Alyea, EP 3rd *et al.* (2011). Interleukin-2 and regulatory T cells in graft-versus-host disease. *N Engl J Med* **365**: 2055–2066.
14. Matsuoka, K, Koreth, J, Kim, HT, Bascug, G, McDonough, S, Kawano, Y *et al.* (2013). Low-dose interleukin-2 therapy restores regulatory T cell homeostasis in patients with chronic graft-versus-host disease. *Sci Transl Med* **5**: 179ra43.
15. Matsuoka, K, Kim, HT, McDonough, S, Bascug, G, Warshauer, B, Koreth, J *et al.* (2010). Altered regulatory T cell homeostasis in patients with CD4+ lymphopenia following allogeneic hematopoietic stem cell transplantation. *J Clin Invest* **120**: 1479–1493.
16. Thornton, AM, Korty, PE, Tran, DQ, Wohlfert, EA, Murray, PE, Belkaid, Y *et al.* (2010). Expression of Helios, an Ikaros transcription factor family member, differentiates thymic-derived from peripherally induced Foxp3+ T regulatory cells. *J Immunol* **184**: 3433–3441.
17. Akimova, T, Beier, UH, Wang, L, Levine, MH and Hancock, WW (2011). Helios expression is a marker of T cell activation and proliferation. *PLoS ONE* **6**: e24226.
18. Himmel, ME, MacDonald, KG, Garcia, RV, Steiner, TS and Levings, MK (2013). Helios+ and Helios- cells coexist within the natural FOXP3+ T regulatory cell subset in humans. *J Immunol* **190**: 2001–2008.
19. Ayyoub, M, Raffin, C and Valmori, D (2013). Comment on "helios+ and helios- cells coexist within the natural FOXP3+ T regulatory cell subset in humans". *J Immunol* **190**: 4439–4440.
20. Dong, S, Maiella, S, Xhaard, A, Pang, Y, Wenandy, L, Larghero, J *et al.* (2013). Multiparameter single-cell profiling of human CD4+FOXP3+ regulatory T-cell populations in homeostatic conditions and during graft-versus-host disease. *Blood* **122**: 1802–1812.
21. MacDonald, KG, Han, JM, Himmel, ME, Huang, Q, Kan, B, Campbell, AI *et al.* (2013). Response to comment on "helios+ and helios- cells coexist within the natural FOXP3+ T regulatory cell subset in humans". *J Immunol* **190**: 4440–4441.
22. Raffin, C, Pignon, P, Celse, C, Debien, E, Valmori, D and Ayyoub, M (2013). Human memory Helios- FOXP3+ regulatory T cells (Tregs) encompass induced Tregs that express Aiolos and respond to IL-1ß by downregulating their suppressor functions. *J Immunol* **191**: 4619–4627.
23. Setoguchi, R, Hori, S, Takahashi, T and Sakaguchi, S (2005). Homeostatic maintenance of natural Foxp3(+) CD25(+) CD4(+) regulatory T cells by interleukin (IL)-2 and induction of autoimmune disease by IL-2 neutralization. *J Exp Med* **201**: 723–735.
24. Malek, TR and Castro, I (2010). Interleukin-2 receptor signaling: at the interface between tolerance and immunity. *Immunity* **33**: 153–165.
25. Pandiyan, P, Zheng, L, Ishihara, S, Reed, J and Lenardo, MJ (2007). CD4+CD25+Foxp3+ regulatory T cells induce cytokine deprivation-mediated apoptosis of effector CD4+ T cells. *Nat Immunol* **8**: 1353–1362.
26. Yu, A, Zhu, L, Altman, NH and Malek, TR (2009). A low interleukin-2 receptor signaling threshold supports the development and homeostasis of T regulatory cells. *Immunity* **30**: 204–217.
27. Lopez-Vergès, S, Milush, JM, Pandey, S, York, VA, Arakawa-Hoyt, J, Pircher, H *et al.* (2010). CD57 defines a functionally distinct population of mature NK cells in the human CD56dimCD16+ NK-cell subset. *Blood* **116**: 3865–3874.
28. Björkström, NK, Riese, P, Heuts, F, Andersson, S, Fauriat, C, Ivarsson, MA *et al.* (2010). Expression patterns of NKG2A, KIR, and CD57 define a process of CD56dim NK-cell differentiation uncoupled from NK-cell education. *Blood* **116**: 3853–3864.
29. Caligiuri, MA, Zmuidzinas, A, Manley, TJ, Levine, H, Smith, KA and Ritz, J (1990). Functional consequences of interleukin 2 receptor expression on resting human lymphocytes. Identification of a novel natural killer cell subset with high affinity receptors. *J Exp Med* **171**: 1509–1526.
30. Freud, AG, Becknell, B, Roychowdhury, S, Mao, HC, Ferketich, AK, Nuovo, GJ *et al.* (2005). A human CD34(+) subset resides in lymph nodes and differentiates into CD56bright natural killer cells. *Immunity* **22**: 295–304.
31. Vosshenrich, CA, García-Ojeda, ME, Samson-Villéger, SI, Pasqualetto, V, Enault, L, Richard-Le Goff, O *et al.* (2006). A thymic pathway of mouse natural killer cell development characterized by expression of GATA-3 and CD127. *Nat Immunol* **7**: 1217–1224.
32. Gasteiger, G, Hemmers, S, Bos, PD, Sun, JC and Rudensky, AY (2013). IL-2-dependent adaptive control of NK cell homeostasis. *J Exp Med* **210**: 1179–1187.
33. Martín-Fontecha, A, Thomsen, LL, Brett, S, Gerard, C, Lipp, M, Lanzavecchia, A *et al.* (2004). Induced recruitment of NK cells to lymph nodes provides IFN-gamma for T(H)1 priming. *Nat Immunol* **5**: 1260–1265.
34. Goldszmid, RS, Caspar, P, Rivollier, A, White, S, Dzutsev, A, Hieny, S *et al.* (2012). NK cell-derived interferon-γ orchestrates cellular dynamics and the differentiation of monocytes into dendritic cells at the site of infection. *Immunity* **36**: 1047–1059.
35. Kerdiles, Y, Ugolini, S and Vivier, E (2013). T cell regulation of natural killer cells. *J Exp Med* **210**: 1065–1068.
36. Sitrin, J, Ring, A, Garcia, KC, Benoist, C and Mathis, D (2013). Regulatory T cells control NK cells in an insulitic lesion by depriving them of IL-2. *J Exp Med* **210**: 1153–1165.
37. Suthanthiran, M, Schwartz, JE, Ding, R, Abecassis, M, Dadhania, D, Samstein, B *et al.*; Clinical Trials in Organ Transplantation 04 (CTOT-04) Study Investigators. (2013). Urinary-cell mRNA profile and acute cellular rejection in kidney allografts. *N Engl J Med* **369**: 20–31.
38. Askarieh, G, Alsiö, A, Pugnale, P, Negro, F, Ferrari, C, Neumann, AU *et al.*; DITTO-HCV and NORDynamIC Study Groups. (2010). Systemic and intrahepatic interferon-gamma-inducible protein 10 kDa predicts the first-phase decline in hepatitis C virus RNA and overall viral response to therapy in chronic hepatitis C. *Hepatology* **51**: 1523–1530.
39. Shimizu, K, Asakura, M and Fujii, S (2011). Prolonged antitumor NK cell reactivity elicited by CXCL10-expressing dendritic cells licensed by CD40L+ CD4+ memory T cells. *J Immunol* **186**: 5927–5937.
40. Weiss, GR, Grosh, WW, Chianese-Bullock, KA, Zhao, Y, Liu, H, Slingluff, CL Jr *et al.* (2011). Molecular insights on the peripheral and intratumoral effects of systemic high-dose rIL-2 (aldesleukin) administration for the treatment of metastatic melanoma. *Clin Cancer Res* **17**: 7440–7450.
41. Panelli, MC, Wang, E, Phan, G, Puhlmann, M, Miller, L, Ohnmacht, GA *et al.* (2002). Gene-expression profiling of the response of peripheral blood mononuclear cells and melanoma metastases to systemic IL-2 administration. *Genome Biol* **3**: RESEARCH0035.
42. Khor, CC, Vannberg, FO, Chapman, SJ, Guo, H, Wong, SH, Walley, AJ *et al.* (2010). CISH and susceptibility to infectious diseases. *N Engl J Med* **362**: 2092–2101.
43. Abbas, AK, Benoist, C, Bluestone, JA, Campbell, DJ, Ghosh, S, Hori, S *et al.* (2013). Regulatory T cells: recommendations to simplify the nomenclature. *Nat Immunol* **14**: 307–308.
44. Canavan, JB, Afzali, B, Scottà, C, Fazekasova, H, Edozie, FC, Macdonald, TT *et al.* (2012). A rapid diagnostic test for human regulatory T-cell function to enable regulatory T-cell therapy. *Blood* **119**: e57–e66.
45. Fauriat, C, Long, EO, Ljunggren, HG and Bryceson, YT (2010). Regulation of human NK-cell cytokine and chemokine production by target cell recognition. *Blood* **115**: 2167–2176.
46. Kauffmann, A, Gentleman, R and Huber, W (2009). arrayQualityMetrics–a bioconductor package for quality assessment of microarray data. *Bioinformatics* **25**: 415–416.
47. Smyth, GK (2004). Linear models and empirical bayes methods for assessing differential expression in microarray experiments. *Stat Appl Genet Mol Biol* **3**: Article3.
48. Benjamini, Y and Hochberg, Y (1995). Controlling the false discovery rate - a practical and powerful approach to multiple testing. *J Roy Stat Soc B Met* **57**: 289–300.